Proceeding of the IEEE
International Conference on Robotics and Biomimetics
Dali, China, December 2019

A Design For An Exoskeletal Device With Reduced Reliance On Joint Alignment

Nicholas Moser and Tim C. Lueth, *Senior Member, IEEE*
Institute for Microtechnology and Medical Device Technology
Technical University of Munich
Boltzmannstrasse 15, 85748 Garching, Germany
nicholas.moser@tum.de

***Abstract*— As robotic exoskeletons begin to find more use in the areas of medicine and rehabilitation, efforts to improve comfort and reduce the chance of injury for wearers have resulted in the development of joint mechanisms with extra passive degrees of freedom. The added redundancy in such mechanisms enables the system to accommodate for joint axis misalignments between the exoskeleton and the human skeleton, as well as deviations from ideal circular motion that are inherent in normal human body motion. However, proper measurement of joint positions and torques, and by extension proper position and impedance control of the exoskeleton still relies on the approximate alignment of these joint axes. This paper presents a method for such a system to calculate the pose and torque about a human elbow joint for a wider variety of possible mounting positions. Using the developed calibration procedure, the main joint of the exoskeleton can be located as much as 110 mm away from the elbow and still position the elbow to within 10 degrees of a given flexion angle and measure torques to within 13 percent of the actual value. An elbow exoskeleton was developed employing this system and tested for comfort. The wearer was able to comfortably move their elbow in any desired motions using the device's passive mode. These results demonstrate the feasibility of using such a system on a robotic rehabilitation device and open up more possibilities for future exoskeleton designs not limited by joint placement.**

***Index Terms*— rehabilitation robotics, medical robotics, robot kinematics, exoskeletons, pose estimation**

I. Introduction

Exoskeletons today find many applications in industry and medicine [1], [2]. Active exoskeletons, i.e. ones that are powered by a motor or some other actuator, can be used to help users lift heavy loads [3], assist disabled wearers in performing normal activities of daily living [4], and aid in rehabilitation programs [5], [6]. For some applications, such as certain rehabilitation programs, the assistive device can be anchored to the floor with only the end effector attached to the person, allowing the chosen body part to be moved in Cartesian space, but without regard to the pose of the rest of the body [7]. For other applications which involve moving about in a space, or in instances where specific joint poses are desired, this strategy does not work, and the exoskeleton must be anchored somewhere on the body and move the other limbs relative to that [5]. It is from here that the problem of joint misalignment arises.

In their simplest form, exoskeletons move human joints by attaching to two separate parts of the body, and bending about a joint whose axis of rotation is in line with the human joint's axis of rotation [8]. For example, to bend a person's elbow, a device anchored to the upper arm can attach to the forearm and move it in a circular path relative to the upper arm. However, if the respective rotational axes are not aligned, there is a mismatch between the motion of the exoskeleton and the motion of the human limb. This can arise as a result of misaligning the device while putting it on [9], but also occurs because the center of rotation (COR) of a human joint will tend to change throughout the course of a movement [10]. The first problem can be fixed, or at least mitigated, by taking extra time and care when first attaching such a device to ensure that the alignment is perfect [9], but this is still problematic since the COR of human joints is not directly observable. Solving the second problem generally involves the development of a more complex mechanical joint to better approximate the true motion of the anatomical joint [11], [12].

One proposed solution to both of these problems is to add additional, passive joints in series between the actuated exoskeleton joint and the attachment point of the exoskeleton to the body [6]. The resulting mechanism is an underactuated multi-degree-of-freedom system whose end-effector (which attaches to the limb being moved) is able to precisely match the natural motion of the limb irrespective of whether the axis of the main joint is properly aligned or not. Schiele and van der Helm [6] employed this mechanism on an upper-limb rehabilitation robot, and further researchers have used similarly inspired mechanisms on other upper-limb rehabilitation exoskeletons [5], [13], as well as in lower limb exoskeletons [14].

Although from a kinematic perspective such devices do not need to be specially aligned, they still rely on the proximity of the mechanical joint to the anatomical joint in order to approximate the pose of the human limb. The authors of this paper have conceived a system where this is not necessary. In fact, the prototype developed to illustrate the functionality of this system does not even allow the main mechanical axis and the elbow axis to be aligned. Since these axes must be so far removed from each other, the control software employed on this device must compensate for this when extrapolating joint position data. If such a system can still perform reliably in terms of positioning accuracy and force transfer, it would allow more flexibility in the choice of motor placement when

978-1-7281-6321-5/19//$31.00 ©2019 IEEE

designing other such systems.

Here the authors present a novel application of the aforementioned mechanism by designing it in conjunction with a software tool to compensate for discrepancies between the elbow angle and motor angle when measuring position. It is here put into use as an actuator for the elbow joint on an upper limb exoskeleton. Even though the elbow is generally modelled as a simple rotational joint, in reality it also displays measurable deviations from this behavior [15], so an elbow exoskeleton can be improved upon with the use of such a mechanism. It should be noted that this device does not provide support to the elbow joint, but rather affords the ability to apply torques about the elbow and position the forearm at specific angles in relation to the upper arm.

In rehabilitation applications, it is not as important to have high accuracy joint positioning [5]. Therefore, an exoskeletal system able to position a human elbow within 10° of a desired position will be considered sufficient for these purposes. This level of accuracy also serves a safety purpose. By being able to detect or otherwise discern the position of the anatomical joints, the system will be able to employ proper joint limits and prevent the arm from hyperextending.

II. Materials and Methods

The proposed mechanism for an underactuated multi-degree-of-freedom elbow joint consists of an actuated main rotational joint, a passive translational joint, and a passive rotational joint in series. This three-degree-of-freedom (3DOF) mechanism was designed, manufactured, and employed on an elbow exoskeleton to illustrate the functionality.

A. Device Construction

The bulk of the device consists of three separate semicircular arm cuffs (two for the upper arm and one for the forearm). The two upper arm cuffs are rigidly connected with a metal plate; the distance between the cuffs is adjustable to fit different arm lengths. The single motor on the device is mounted on the upper arm cuff closest to the elbow and the output connects to two parallel anodized aluminum rods that swing around the motor axis. The forearm cuff has a housing for a radial ball bearing. An aluminum shaft extends out from here in a radial direction from the cuff and connects to two RJUM-01-10 drylin linear bearings (igus GmbH, Cologne, Germany). These bearings are able to slide along the aluminum rods extending out from the upper arm cuff and can rotate relative to the forearm. The complete device is shown in Fig. 1.

The majority of the device was manufactured using selective laser sintering (SLS) of the polymer PA2200 (EOS, Krailing, Germany). This process of fusing together layers of plastic powder allows one to create intricate stiff or flexible structures quickly and easily [16]. The three cuffs, the right angle connector between the motor and the aluminum rods, and the connectors between the linear bearings and the aluminum shaft connecting to the forearm cuff are all printed using SLS. For added comfort when wearing the device, 4 mm thick neoprene

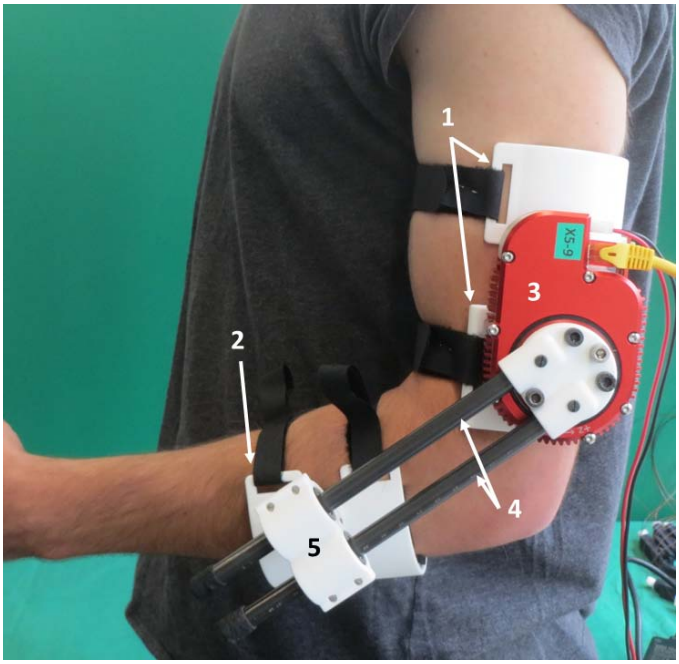

Fig. 1. The assembled elbow exoskeleton consisting of (1) upper arm cuffs, (2) forearm cuff, (3) series elastic motor, (4) aluminum rods, and (5) linear bearings in a housing. The housing for the linear bearings is connected to a radial ball bearing housed in the forearm cuff, which allows it to rotate relative to the forearm cuff.

padding is attached to the each of the cuffs via hook-and-loop fasteners. Altogether, the device has a mass of 739.9 g.

B. Series Elastic Actuation

The actuator used on the device is a X5-9 actuator from HEBI Robotics (Pittsburgh, USA). This module is a self-contained series elastic actuator (SEA), so the output of the actuator is connected to the motor itself by a spring with a known spring constant. SEAs can offer several different advantages in robotic systems, such as providing a source of mechanical compliance. The spring in this particular module is too stiff to provide a significant amount of compliance for this application, but together with the built-in encoders, it does act as an integrated torque sensor. This is a useful feature for applications such as rehabilitation where it is desirable to use impedance control to apply varying degrees of resistance or assistance to a patient's limb movements. Having a stiff spring also increases the positioning accuracy of the actuator compared to an SEA with a lower spring stiffness.

There are several APIs published by HEBI that can be used to operate these modules. MATLAB (Mathworks, Natick, USA) was selected to be used on this device.

C. Kinematic System

The resulting device has kinematic complexities not present in a traditional elbow exoskeleton. When the COR of the exoskeleton lines up with the COR of the elbow, it is trivial to measure the position of the elbow (which matches the positioning of the exoskeleton) and the torque applied about

the elbow (which matches the torque applied about the exoskeleton joint). However, in the system presented here, there is a significant offset between the COR of the motor and the COR of the elbow. The extra degrees of freedom present in the design ensure that the device will still be able to match the movement of the arm no matter how it is positioned, but only the position of one of the rotational joints is known, so on this information alone it is impossible to know exactly how the device is positioned. However, the exoskeleton also forms a closed loop kinematic chain with the arm which still has only one degree of freedom at the elbow, so by knowing how the two are connected, the position and torque information gathered by the motor can be used to extrapolate the position and torque about the elbow.

Assuming that the motor axis and the elbow axis are parallel, i.e. the movement of the exoskeleton and the movement of the elbow are in the same plane, determining the elbow angle θ_e from the motor angle θ_m can be treated as a 2D problem. We start by looking at the triangle defined by the motor COR, the elbow COR, and the point at which the mechanism intersects the forearm (labeled as M, E, and P respectively in Fig. 2). The angle β between the vector $\vec{E}$ from M to E, and the vector $\vec{P}$ from M to P along the arm of the exoskeleton can be defined as

$$\beta = \theta_m - \gamma, \tag{1}$$

where γ is the angle between $\vec{E}$ and the x-axis of the motor reference frame. Defining the lengths $\{r_0, r_1, r_2\}$ as

$$r_0 = \|\vec{E}\|, \tag{2}$$
$$r_1 = \|\vec{P}\|, \tag{3}$$
$$r_2 = \|\vec{P} - \vec{E}\|, \tag{4}$$

the length of the segment from the motor to the forearm (r_1) can be written as

$$r_1 = r_0 \cos(\beta) + \sqrt{r_2^2 - r_0^2 \sin^2(\beta)}. \tag{5}$$

Finally, θ_e can be found by solving

$$\theta_e + \psi = -\text{atan2}(y_p - y_e, x_p - x_e), \tag{6}$$
$$\theta_e \quad\quad = -\text{atan2}(y_p - y_e, x_p - x_e) - \psi, \tag{7}$$

where

$$x_p = r_1 \cos(\theta_m), \tag{8}$$
$$x_e = r_0 \cos(\gamma), \tag{9}$$
$$y_p = r_1 \sin(\theta_m), \tag{10}$$
$$y_e = r_0 \sin(\gamma). \tag{11}$$

The torque is calculated by analyzing the forces experienced at the forearm connection point. Let F be the magnitude of the force on the forearm applied by the exoskeleton in the direction perpendicular to the forearm. Then the torque that such a force would induce about the elbow COR (T_2) would be

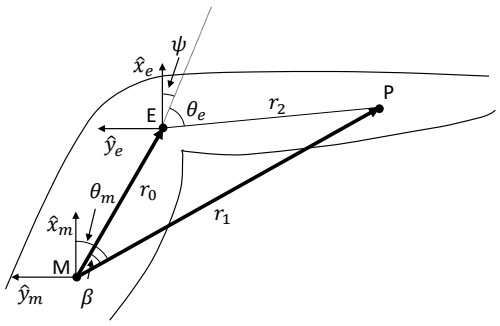

Fig. 2. Schematic of the kinematic system showing the geometry of the exoskeleton mechanism and its interface with a human arm. The mechanism consists of a motorized joint with position defined as θ_m, a passive translational joint with position defined as r_1, and a passive rotational joint where it intersects the forearm at P.

$$T_2 = F r_2, \tag{12}$$

and the motor torque (T_1) needed to apply this force can be expressed as

$$T_1 \frac{\sqrt{r_2^2 - r_0^2 \sin^2(\beta)}}{r_2} = F r_1. \tag{13}$$

By combining (12) and (13) above, we arrive at,

$$F = \frac{T_2}{r_2} = T_1 \frac{\sqrt{r_2^2 - r_0^2 \sin^2(\beta)}}{r_1 r_2}, \tag{14}$$
$$T_2 = T_1 \frac{\sqrt{r_2^2 - r_0^2 \sin^2(\beta)}}{r_1}. \tag{15}$$

θ_m is measured by the encoder, but to use these equations, it is still necessary to know the position of the motor axis relative to the elbow axis, $\vec{E}$; the distance from the elbow axis to the forearm cuff, r_2; and the reference angle, ψ, between the x-axis and the fully extended position of the forearm. Since all of these parameters remain constant as long as the exoskeleton remains on the arm, it is possible to learn these values from a calibration procedure (detailed in the next section) performed when the device is first put on. Once these parameters have been determined, they can be used in the formulas above to find the position and the torque about the arm.

D. Calibration

The calibration of the exoskeleton involves four measurements. First, the elbow is held at a 90° angle. From there, the motor angle and the distance from the motor to the forearm

cuff is measured. The motor angle can be measured by the encoder on the motor, but there is no way for the software to directly read the distance measurement; therefore, a ruler was etched into the aluminum rod, so that with the arm still held at the 90° position, the position of the forearm cuff can easily be read off and manually entered into the calibration program. The same procedure must then be repeated with the arm held straight out at the 0° position.

With these measurements it is then possible to extrapolate the parameters required to calibrate the device. Each angle and distance combination measured above defines a point in 2D relative to the motor reference frame. Assuming that the elbow motion causes the forearm cuff to trace out a circle centered on the elbow COR, we now have the coordinates of two points on a circle separated by a 90° arc. The center of this circle corresponds to the COR of the elbow, which defines $\vec{E}$, and the radius corresponds to the distance from the COR to the forearm cuff, which defines r_2. From the two possible solutions for the location of the elbow COR, the one closest to the motor is selected since, for this application, it is assumed that the elbow will lie in between the motor and the forearm. The reference angle ψ can then be calculated based on the 0° angle/distance measurement. Once measured, these values will remain the same as long as the exoskeleton stays on. If it is taken off or readjusted, the calibration procedure will have to be run again in order to determine the proper calibration parameters.

E. MATLAB Application

To aid in the use of this device, a MATLAB application has been developed which replicates some of the functionality of the Scope UI from HEBI. Similar to Scope, with this MATLAB UI one can set a desired position, velocity, or force to be targeted by the motor for a given amount of time, and also set position limits for the motor. When not taking any other actions, the app will display the real-time measurements of the position, velocity, and torque measured by the motor. There is also an option to record motor data and save it to a log file on the disk as well as view data from saved log files, which can be done in conjunction with any other action.

In addition, the app has some application specific functionality that is not covered by Scope. This includes the ability to select which arm the exoskeleton is being worn on, which automatically selects position limits to prevent hyperextension of the elbow. The default position limits are -10° and 115°. It can also reproduce a trajectory recorded in a log. This means that in a rehabilitation setting, a therapist can set the device to record and manually move the patient's arm in a desired motion. Once done, the app can be used to easily reproduce the motion as many times as desired. There is also a stop button to stop the motor during any of its routines.

The app can also take care of calibrating the exoskeleton. Once it is connected and attached to the arm, the calibrate button just needs to be pushed and the app will guide the user through moving their arm into the proper positions and entering the two distance measurements required for the calibration. Once the exoskeleton is calibrated, position, velocity, and torque commands from the app are carried out with reference to the elbow and not the motor. For example, before calibration, commanding a position of 60° would cause the motor to move to the 60° position; after calibration, commanding a position of 60° will cause the motor to move the arm to the 60° position based on the calibration data.

III. Experiments

Several experiments were carried out in order to test the functionality of various parts of the exoskeleton system. Four main things had to be tested: (1) the calibration procedure was run for several different known configurations in order to test the accuracy of the calculation, (2) the positioning accuracy of the exoskeleton was tested, (3) the ability to accurately identify a given torque was tested, and (4) the comfort and wearability of the entire system as determined by a healthy subject was tested. The first three tests were performed on the mechanism directly and not on the full exoskeleton attached to an arm. Test stands were designed with idealized rotational "elbow joints" in order to more easily measure joint positions and apply torques to characterize the performance of the system.

A. Calibration

For the calibration experiment, the motor was removed from the upper arm cuff and attached to a platform whose position on the test stand could be adjusted. The rod extended from the motor as usual, with the linear bearing able to slide along it. The bearing was then affixed to a rotatable arm attached to an encoder. This "arm" would simulate an idealized human forearm in this experiment. The arm had a series of regularly spaced attachment points for the bearing, to represent different distances of the forearm cuff from the

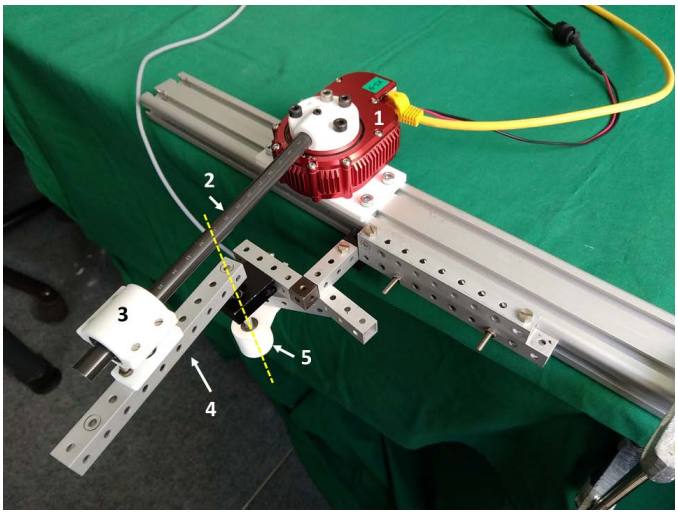

Fig. 3. Setup including (1) the motor mounted on a sliding platform, with (2) the aluminum rod and (3) linear bearing still attached. The bearing is now connected to (4) the idealized "forearm" which can swivel about the yellow axis and is connected to (5) an encoder. This setup was used for both the calibration and positioning experiments.

elbow COR. With this setup, as shown in Fig. 3, the stripped down device could be attached at different known mounting positions and the calibration procedure performed. The results from the calibration were compared to the previously measured values to get a measurement of accuracy for the procedure.

Trials were performed for three different motor positions and two different forearm attachment positions for a total of six trials. Each trial began by attaching the motor and the linear bearing to the proper positions and running the calibration procedure. The program would then output the calculated values which could then be compared to the true values. Fig. 4 shows the 2D positions of the elbow COR as computed by the calibration program relative to the measured position, which is represented by the origin. The X- and Y-axes shown are in line with the motor reference frame but shifted to the elbow COR position. All calculated positions were accurate to within 8 mm. Fig. 5 also shows how far off the forearm lengths calculated by the calibration were from the measured lengths. The calculated lengths are all within 1.5 mm of the measured lengths with a mean offset of 0.8 mm.

While the errors from the calibration results seem low, the real measure of interest is how these errors affect the ability of the device to measure position accurately. Table I shows how the errors calculated previously in the calibration should propagate into errors in positioning. For evenly spaced elbow angles from 0° to 90°, the mean error in the position that would be measured by the device, given that it was calibrated with the results described above, is shown. The mean error is less than 1° until an elbow angle of 90° is reached, but it is still low enough to make little difference in most applications.

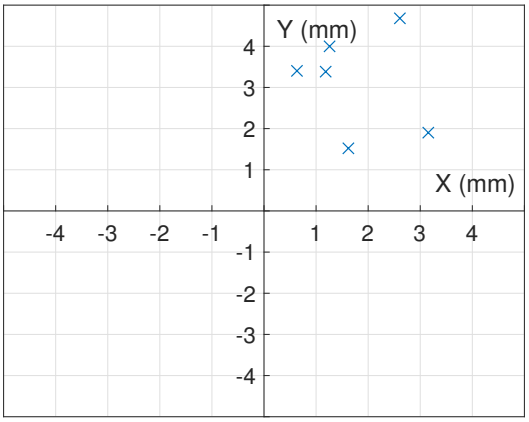

Fig. 4. Shows the position of the elbow COR as calculated by each of the calibration procedures performed. The computed results are plotted relative to the actual position of the elbow COR–in this case represented by the origin. The algorithm consistently calculates the position to within 8 mm and within the first quadrant.

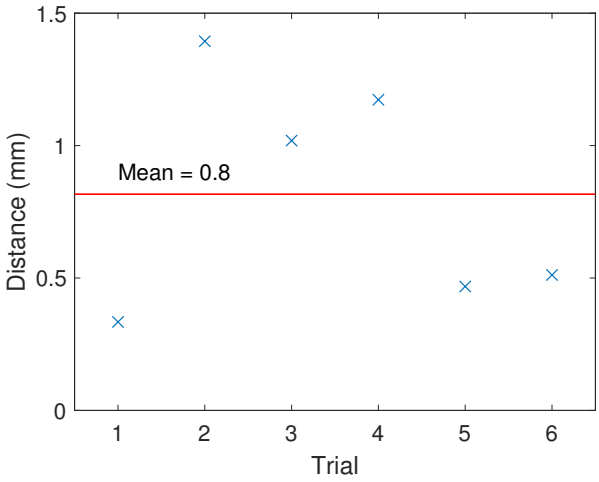

Fig. 5. Shows the position of the forearm cuff along the forearm as calculated by each of the calibration procedures performed. The absolute error in the computed distances for each trial are plotted. The algorithm consistently calculates the position to within 1.5 mm.

TABLE I
THEORETICAL CHANGES IN POSITIONING ACCURACY RESULTING FROM CALIBRATION ERRORS

Angles (deg)	Mean Difference (deg)	Standard Deviation of Difference
0	0.0	0.0
15	-0.2	0.2
30	-0.3	0.4
45	-0.3	0.5
60	-0.1	0.6
75	0.5	0.6
90	3.0	2.3

B. Positioning

The experiment to test the positioning accuracy of the exoskeleton mechanism was performed in conjunction with the calibration experiment, so the same setup was used for both. The test stand had an AS5040 10-bit rotary encoder (ams AG, Premstaetten, Austria) attached to the axle of the simulation arm in order to get an accurate measurement of the ”true” position of the arm. The arm position could then be measured with an accuracy of 0.35°. Immediately after performing the calibration procedure for each configuration as described above, the exoskeleton was given position commands from 0° to 90° in 15° increments. After sending each command, the measurement from the encoder would be recorded before moving on to the next position command. This would continue over the whole 90° range, then start over and repeat in order to take into account the repeatability of the process.

The results of these experiments are shown in Table II. The mean error in the position across every trial as measured by the encoder is given for each elbow angle that was commanded and a 95% confidence interval is presented. The errors are larger in magnitude than those predicted by the calibration, which could stem from inaccuracies in the PD control scheme used

TABLE II

POSITIONING ACCURACY EXPERIMENTAL RESULTS

Angles (deg)	Mean Difference (deg)	95% Confidence Interval	
		Min	Max
0	0.8	0.1	1.5
15	0.4	0.0	0.8
30	-0.1	-0.4	0.2
45	-1.0	-1.4	-0.6
60	-2.1	-3.0	-1.3
75	-3.9	-5.4	-2.3
90	-6.5	-9.2	-3.8

by the motor, but the errors still manage to stay below 10° in magnitude, implying that the mechanism itself is capable of a positioning accuracy befitting the needs of a rehabilitation program.

C. Torque

The torque measurement experiments consisted of two parts. The first part aimed to evaluate how accurately the torque sensor of the HEBI motor could measure torques on its own. This was done by detaching the motor from the exoskeleton with only the rod still attached and mounting it to a stationary base. Loads from 0 to 60 N were applied at distances of 11.3 cm and 18.3 cm along the rod, as measured by a 200 N spring scale with 2 N resolution (Pesola, Schindellegi, Switzerland), while the motor was commanded to hold a horizontal position using a PID control strategy. Torque measurements were read at a rate of 100 Hz and averaged over a 3 second window after reaching equilibrium in order to get a single torque measurement. After taking into account the weights of the exoskeleton parts and the hanging scale itself, a series of applied torques ranging from 0 to 12 Nm was achieved and measured as shown in Fig. 6.

The second part of the torque experiments were performed using once again a test arm with a known weight. The motor was once again mounted and the linear bearings were attached to the test arm at three different positions as in Fig. 7. The calibration procedure was performed for each configuration, then the motor was commanded to hold the test arm in a horizontal position, equivalent to a 90° elbow joint angle, while forces from 0 to 30 N were applied to the end of it. As before, torque measurements were averaged over a 3 second window after an equilibrium state was reached. The results, shown in Fig. 8, show a tendency for the system to underestimate the actual torque applied, with the error increasing linearly with torque, which is the expected behavior for a system that has errors in calibration. The average measured torque was 7.9% below the true value with a 95% confidence interval of between 3.6% to 12.2% below the true value. At the low torques tested here, the error is still relatively low, but for higher torque applications, better solutions will have to be investigated.

D. Integrated Experience

As a final test of the system, the mechanism was attached to the 3D printed arm cuffs to form a full exoskeleton. It was donned by a healthy male who used it in several different modes. While in zero-force mode, the user was able to move his arm around freely and comfortably, and when the device was commanded to move to and hold a given position, the user was unable to move his elbow. The entire device was easy for the user to put on by themselves in under a minute. Further in-depth experiments to gauge how well the positioning accuracy seen in the earlier experiments translates onto a human arm must still be performed, but the basic feasibility of using the proposed system on an exoskeleton has been demonstrated.

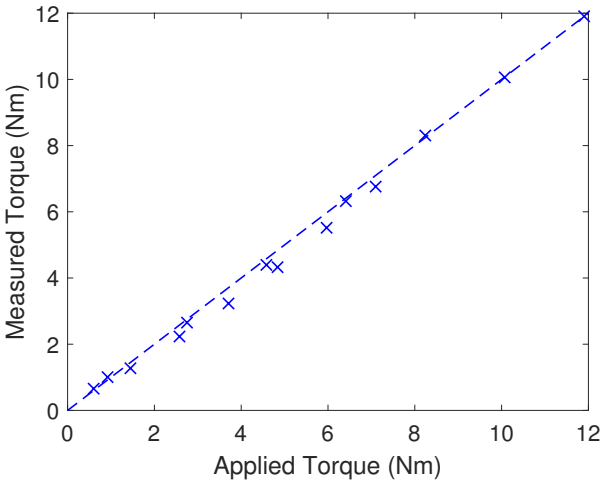

Fig. 6. Plot showing the torques measured by the HEBI module, relative to the actual torque applied to the arm. The dashed line is a reference for equal torques.

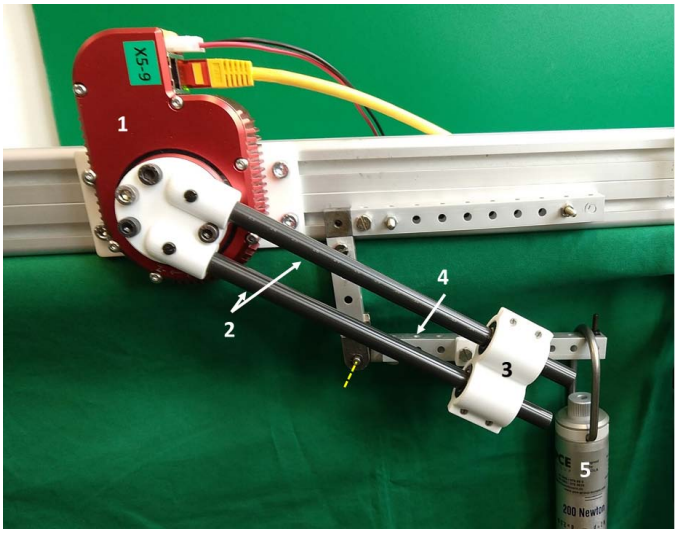

Fig. 7. Setup for the torque experiments including (1) the motor mounted on a stationary base with (2) the aluminum rods and (3) linear bearings. The bearings are connected to (4) the idealized "arm" which is held at a 90° angle as shown. Force is applied to (5) the spring scale shown to generate a torque about the "elbow" axis shown in yellow.

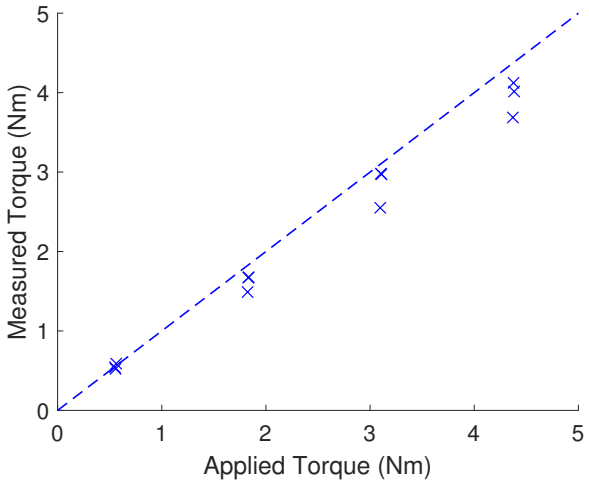

Fig. 8. Plot showing the torques measured by the device, relative to the actual torque applied to the arm. The dashed line is a reference for equal torques.

IV. Conclusion

The authors have presented a novel robotic elbow exoskeleton with the capability of separating the main axis of rotation of the mechanism from the anatomical axis of rotation. Although the physical mechanism employed on this device is not new, and has in fact been used on several elbow joints before now, the ability to locate the main center of rotation of the actuator a significant distance from the actual elbow has now been realized. This method of calibrating the device to determine its location on the arm allows it to convert the position and torque measurements taken with respect to the motor into position and torque measurements with respect to the elbow. While far from a finished product, the device demonstrates the ability to relocate not only the motors but the actual joints on an exoskeleton and still achieve comfortable motion precise enough for robotic rehabilitation. Future work will focus on further increasing the fidelity of these measurements, increasing the torque output to cover a larger range of human strength capabilities, and further testing its performance with human subjects.

References

[1] M. P. De Looze, T. Bosch, F. Krause, K. S. Stadler, and L. W. O'Sullivan, "Exoskeletons for industrial application and their potential effects on physical work load," *Ergonomics*, vol. 59, no. 5, pp. 671–681, 2016.

[2] R. Gopura, K. Kiguchi, and D. Bandara, "A brief review on upper extremity robotic exoskeleton systems," *2011 6th international Conference on Industrial and Information Systems*, pp. 346–351, 2011.

[3] Z. Luo and Y. H. Yu, "Wearable stooping-assist device in reducing risk of low back disorders during stooped work," *2013 IEEE International Conference on Mechatronics and Automation*, pp. 230–236, 2013.

[4] M. Gandolla, A. Costa, L. Aquilante, M. Gfoehler, M. Puchinger, F. Braghin, and A. Pedrocchi, "Bridge — behavioural reaching interfaces during daily antigravity activities through upper limb exoskeleton: Preliminary results," in *2017 International Conference on Rehabilitation Robotics (ICORR)*, July 2017, pp. 1007–1012.

[5] Z. Song and S. Guo, "Design process of exoskeleton rehabilitation device and implementation of bilateral upper limb motor movement," *Journal of Medical and Biological Engineering*, vol. 32, no. 5, pp. 323–330, 2012.

[6] A. Schiele and F. C. Van Der Helm, "Kinematic design to improve ergonomics in human machine interaction," *IEEE Transactions on Neural Systems and Rehabilitation Engineering*, vol. 14, no. 4, pp. 456–469, 2006.

[7] S. J. Spencer, J. Klein, K. Minakata, V. Le, J. E. Bobrow, and D. J. Reinkensmeyer, "A low cost parallel robot and trajectory optimization method for wrist and forearm rehabilitation using the wii," in *2008 2nd IEEE RAS EMBS International Conference on Biomedical Robotics and Biomechatronics*, Oct 2008, pp. 869–874.

[8] S. Bai, S. Christensen, and M. R. U. Islam, "An upper-body exoskeleton with a novel shoulder mechanism for assistive applications," *2017 IEEE International Conference on Advanced Intelligent Mechatronics (AIM)*, pp. 1041–1046, 2017.

[9] A. H. A. Stienen, E. E. G. Hekman, F. C. T. van der Helm, and H. van der Kooij, "Self-aligning exoskeleton axes through decoupling of joint rotations and translations," *IEEE Transactions on Robotics*, vol. 25, no. 3, pp. 628–633, June 2009.

[10] A. Forner-Cordero, J. L. Pons, E. Turowska, A. Schiele, J. Baydal-Bertomeu, D. Garrido, F. Mollá, J. Belda-lois, R. Poveda, and R. Barberá, "Kinematics and dynamics of wearable robots," *Wearable robots: biomechatronic exoskeletons*, pp. 47–85, 2008.

[11] C. M. Hein, P. A. Maroldt, S. V. Brecht, H. Oezgoecen, and T. C. Lueth, "Towards an ergonomic exoskeleton structure: Automated design of individual elbow joints," *2018 7th IEEE International Conference on Biomedical Robotics and Biomechatronics (Biorob)*, pp. 646–652, 2018.

[12] N. Vitiello, T. Lenzi, S. Roccella, S. M. M. De Rossi, E. Cattin, F. Giovacchini, F. Vecchi, and M. C. Carrozza, "Neuroexos: A powered elbow exoskeleton for physical rehabilitation," *IEEE Transactions on Robotics*, vol. 29, no. 1, pp. 220–235, Feb 2013.

[13] N. Jarrasse and G. Morel, "Connecting a human limb to an exoskeleton," *IEEE Transactions on Robotics*, vol. 28, no. 3, pp. 697–709, 2012.

[14] K. Junius, M. Degelaen, N. Lefeber, E. Swinnen, B. Vanderborght, and D. Lefeber, "Bilateral, misalignment-compensating, full-dof hip exoskeleton: design and kinematic validation," *Applied Bionics and Biomechanics*, vol. 2017, 2017.

[15] E. Chao and B. Morrey, "Three-dimensional rotation of the elbow," *Journal of Biomechanics*, vol. 11, no. 1, p. 73, 1978.

[16] D. B. Roppenecker, A. Pfaff, J. A. Coy, and T. C. Lueth, "Multi arm snake-like robot kinematics," in *2013 IEEE/RSJ International Conference on Intelligent Robots and Systems*, Nov 2013, pp. 5040–5045.